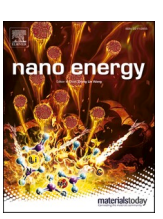
FISEVIER

Contents lists available at ScienceDirect

Nano Energy

journal homepage: http://www.elsevier.com/locate/nanoen



Full paper



Tuning Zn²⁺ coordination environment to suppress dendrite formation for high-performance Zn-ion batteries

Runzhi Qin ¹, Yuetao Wang ¹, Mingzheng Zhang ¹, Yan Wang, Shouxiang Ding, Aoye Song, Haocong Yi, Luyi Yang, Yongli Song, Yanhui Cui, Jian Liu, Ziqi Wang, Shunning Li ^{*}, Qinghe Zhao ^{*}, Feng Pan ^{*}

School of Advanced Materials, Peking University Shenzhen Graduate School, Shenzhen 518055, PR China

ARTICLE INFO

Keywords: Zn ion batteries Ethylene glycol Coordination environment Dendrite suppression

ABSTRACT

The short-circuit issue induced by Zn dendrite growth restricts the commercialization of rechargeable aqueous Zn-ion batteries (ZIBs). Herein, ethylene glycol (EG), a representative of dihydric alcohols, is applied in the aqueous electrolyte to inhibit the detrimental dendrite growth on Zn anode. Our work demonstrates a uniform Zn plating/stripping in $\rm H_2O/EG$ hybrid electrolyte with cycling lifespan of up to 2668 h at 0.5 mA cm⁻², which is made possible by the substitution of EG for $\rm H_2O$ in the solvation sheath of $\rm Zn^{2+}$ ions. Such a change in the coordination environment of $\rm Zn^{2+}$ gives rise to decreased diffusivity of the ions and increased over-potential for nucleation, further resulting in even deposition morphology rather than large-scale dendrites. Side reactions are also circumvented by the formation of hydrogen bonds. All these aspects work in synergy to promote the cyclability of the assembled full battery. The low-cost aqueous electrolyte identified in this work opens up new opportunities for manipulating the coordination environments of $\rm Zn^{2+}$ ions and optimizing the Zn deposition morphology during the design of high-performance ZIBs.

1. Introduction

In recent years, the ever-growing development of green energies (e. g., solar, wind, etc.) calls for reliable and high-performance grid energy storage systems. Aqueous zinc ion batteries (ZIBs) have been widely recognized as promising candidates for future energy applications due to the advantages of zinc anode, including high gravimetric capacity (820 mAh g⁻¹), high volumetric capacity (5585 mAh cm⁻³), low redox potential (-0.762 V vs the standard hydrogen electrode), high abundance and low toxicity [1-3]. Efforts towards the design of reversible ZIBs were initiated in late 1990 s [4] and have now led to numerous studies focusing on the exploration of advanced cathode materials, such as MnO₂ [5–7], V₂O₅ [8], Zn_xV₂O₅ [9], and Prussian blue [10]. In contrast to the fast progress of ZIB cathodes, it still remains a major issue that the zinc anode tends to form dendrites and trigger side reactions such as hydrogen evolution reaction (HER) during cycling. The dendrite formation is the major obstacles for the commercialization of metal anodes [11]. During plating process, Zn²⁺ ions are expected to deposit at the existing protuberances owing to their high surface energy [12,13], thus resulting in the persistent growth of Zn dendrites. Not only can the uncontrolled Zn dendrites pierce through the separator and bridge the cathode and anode, eventually leading to short-circuit failure [14], but their friable tips are also likely to rupture and turn into inert "dead" Zn, which will lower the Coulombic efficiency (CE) of the full battery. Therefore, it is strongly needed to develop strategies for modulating the kinetics of Zn electrodeposition so as to obtain a homogeneous Zn nucleation and inhibit dendrite formation.

It is undeniable that many attempts, including surface coating [15–17], structural transformation [18,19], alloying [20,21], electrolyte additive [22,23], "water-in-salt" design [24,25], etc., contribute significantly to the improvement in electrochemical performance of the Zn anode. The underlying goals are to average the electric field, to optimize the Zn^{2+} ion flux, or to create a physical barrier for blocking the dendrite. Nevertheless, most of the approaches are either too complicated or too costly. Since the direct optimization of the anode is generally tedious and expensive, tuning the electrolyte would be a more desirable direction, and the understanding of coordination environment of Zn^{2+} is critical to this endeavor [26]. Recently, it has been recognized

E-mail addresses: lisn@pku.edu.cn (S. Li), zhaoqh@pku.edu.cn (Q. Zhao), panfeng@pkusz.edu.cn (F. Pan).

^{*} Corresponding authors.

¹ R. Qin, Y. Wang, and M. Zhang contribute equally to this work.

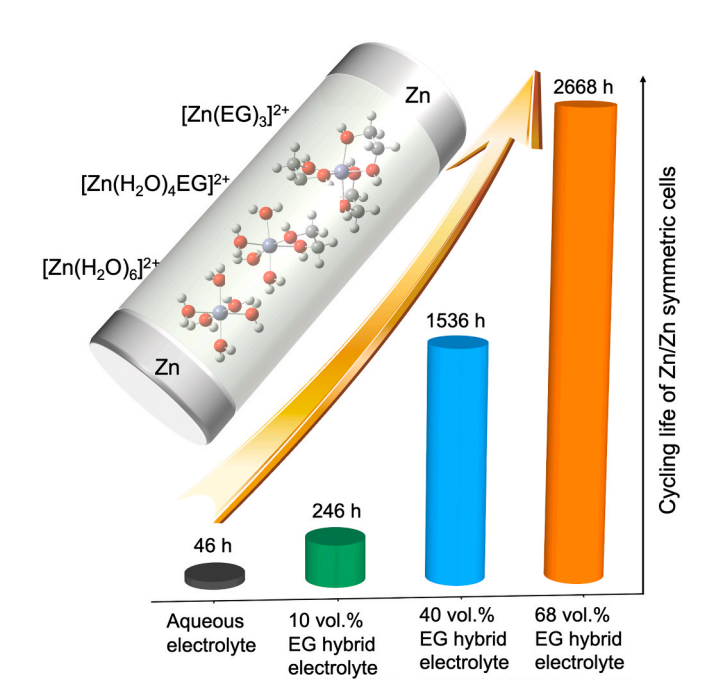
that the $\rm Zn^{2+}$ -solvation sheath in concentrated electrolytes can be effectively altered (e.g. $\rm [ZnCl_4]^2$ - in 30 mol kg $^{-1}$ ZnCl $_2$ electrolyte [24], and Zn(TFSI) $_m(\rm H_2O)_n$ clusters in 1 mol kg $^{-1}$ Zn(TFSI) $_2$ +20 mol kg $^{-1}$ LiTFSI electrolyte [25]), and correspondingly, a smooth morphology of Zn deposits is attained. The key to dendrite-free plating/stripping of Zn rests on the displacement of coordinating H $_2$ O around Zn $^{2+}$ by specific kinds of anions and molecules such that the Zn $^{2+}$ desolvation energy is increased moderately, which enables the kinetics for homogeneous Zn deposition. Although the exorbitant price of the proposed electrolytes in previous studies restricts their potential for practical application, the idea of manipulating the Zn $^{2+}$ coordination environment for purposes of dendrite suppression could provide inspiration for the exploitation of electrolytes with low production costs.

Herein, we report a low-cost aqueous electrolyte consisting of ZnSO₄ and ethylene glycol (EG), which is shown to aid the reversible plating/stripping of $\rm Zn^{2+}$ ions. The cycling lifespan for the bare Zn anode is vastly improved (up to 2668 h at 0.5 mA cm $^{-2}$) with uniform Zn nucleation and growth as accounted for by the modification of $\rm Zn^{2+}$ coordination environment in the electrolyte (Scheme 1). The parasitic reactions at the electrode/electrolyte interface are also mitigated. Full batteries employing this novel electrolyte can offer high capacitance and excellent durability even at low temperatures. This study demonstrates that the incorporation of EG in the electrolyte represents a promising strategy for creating efficient, long-life rechargeable ZIB.

2. Results and discussion

2.1. Enhanced cycling life of Zn/Zn cells with H₂O/EG hybrid electrolyte

In a typical aqueous $ZnSO_4$ electrolyte, the Zn^{2+} ions coordinate with water molecules in the form of $[Zn(H_2O)_6]^{2+}$ [27]. Here, we select the alcohols with abundant hydroxyl groups (similar to water) as solvent additive to tune the coordination of Zn^{2+} . First, by using symmetrical Zn/Zn cells, we compare the performance of different electrolytes incorporating various kinds of alcohols. 3 mol L^{-1} (3 M) $ZnSO_4$ electrolytes with H_2O (90 vol%) and alcohols (10 vol%) are prepared, and the selected alcohols include methanol, ethanol, propy alcohol, ethylene glycol, 1,2-propylene glycol, 1,3-propylene glycol, 1,2-butylene glycol,



Scheme 1. Schematic illustration of coordination state of Zn^{2+} in H_2O/EG hybrid electrolytes, and the effect of EG on the cycling stability of Zn/Zn symmetric cells.

1,3-butylene glycol, glycerol, and diethylene glycol. The corresponding cycling performances at current density of 0.5 mA cm $^{-2}$ are shown in Fig. S1. Zn/Zn symmetric cells with pure 3 M ZnSO₄/H₂O electrolyte fail after 46 h (23 cycles) due to short circuit, which is viewed as the main obstacle for the application of ZIBs [21,27]. Cells with electrolytes containing mono alcohols (methanol, ethanol and propy) survive more cycles (37, 31 and 74, respectively) before failure. Yet, it should be mentioned that propy alcohol could lead to markedly increased overpotential (> 0.1 V). As compared to mono alcohols, polyalcohols are more promising with cycle life extended to beyond 60 cycles. In this study, we select EG as a representative for the polyalcohols for its low price, low toxicity, and ultimate mutual solubility with water.

Electrolytes with different EG concentrations are evaluated. 3 M ZnSO₄ is used due to its improvement in full cell performance as compared with dilute solutions[28]. For 3 M ZnSO₄/ H₂O/ EG hybrid electrolytes, a clear electrolyte is maintained with 4-68 vol% EG, while suspension occurs in 70 vol% EG added electrolyte (Fig. S2). Hence, the EG content in electrolytes is controlled in the range between 0 and 68 vol%. Fig. 1a shows the cycling performance of Zn/Zn symmetric cells at current density of 0.5 mA cm⁻² in 3 M ZnSO₄/ H₂O (0E), 3 M ZnSO₄/ H₂O/ 10 vol% EG (10E), 3 M ZnSO₄/ H₂O/ 40 vol% EG (40E) and 3 M ZnSO₄/H₂O/68 vol% EG (68E) electrolytes. It is found that an increase in EG content can induce a prolonged cycle life, which could yield a maximum of 1334 cycles before short-circuit failure. This trend is valid even at a high current density of 5 mA cm⁻², as shown in Fig. 1b. Although the cycling lifespan of Zn/Zn cell is positively correlated with EG concentration (Fig. 1c), a linear correlation also exists between the over-potential and the EG content in the electrolyte (Fig. 1d), implying an unavoidable link between the smoother Zn deposition and a higher polarization potential. The CE in Zn/Cu cells with different electrolytes is compared in Fig. 1e and S3, where a dramatic increase in CE from 74% to 91% occurs when 10 vol% EG is added into the 0E electrolyte. A suppression of side reactions by EG can be anticipated from the above result. Overall, the impressive cycling performance of EG-containing electrolytes suggests the potential benefits of EG in preventing fast Zn dendrite formation and avoiding competitive side reactions, which places the assembled Zn/Zn cell in this work among the best reported in the literatures (Table S1).

2.2. Suppressed Zn dendrite in H₂O/EG hybrid electrolyte

To provide direct microscopic information on Zn dendrite growth, the morphology of Zn anode is characterized by laser confocal scanning microscope (LCSM) and scanning electron microscopy (SEM). For pristine Zn plate, the altitude intercept on the surface is \sim 5.8 μ m (Fig. S4). As is visible in Fig. 2, a more glabrous Zn deposition is achieved with higher EG concentration in the electrolyte, substantiating our claim that EG can offer the advantage of less tendency for dendrite growth during cycling. The Zn anode in 0E electrolyte exhibits a coarse surface with isolated dendrites of \sim 32.6 µm height after 1 h plating at 0.5 mA cm⁻² (Fig. 2a). In sharp contrast, the altitude intercept is only \sim 32.1 μm in 68E electrolyte after operating for 200 h (Fig. 2f), and this value increases to \sim 47.2 μm after 400 cycles (800 h) (Fig. S5). The SEM image of Zn deposits in 0E electrolyte (Fig. S6) indicates a coralloid structure consisting of crossed branches, which grow and interweave with each other, forming bulk dendrite clusters with lots of voids. In comparison, Zn deposits in 10E and 68E electrolytes are much more uniform and compact with nearly no voids. The dendrites gradually grow during cycling (Fig. S7 and S8), which is well consistent with the LCSM images.

We also noticed that some mini black spots appear inside the white membrane of Zn/Zn cell in 0E electrolyte (Fig. S7a), whose presence corresponds to broken Zn dendrite tips piercing into the membrane [29], as evidenced by optical microscope image (Fig. S9). For Zn anodes cycled for 40 h in 10E and 68E electrolytes, no visible black spots are detected (Fig. S7c, S7e, and S10), which corroborates with our observation of suppressed dendritic growth in both electrolytes. In XRD

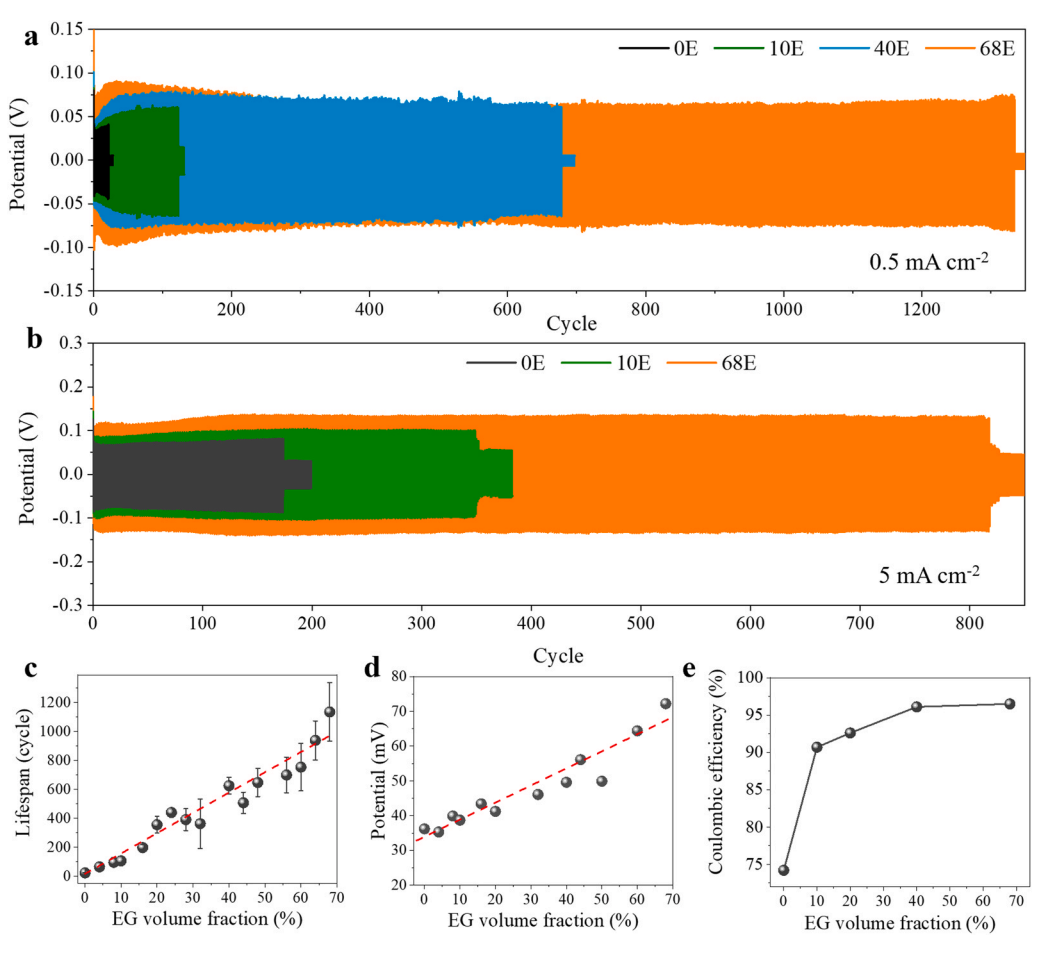


Fig. 1. a) Long-term galvanostatic cycling performances of Zn/Zn cells in 3 M ZnSO₄ $\rm H_2O/EG$ hybrid electrolytes with various EG contents (0, 10, 40, 68 vol%) at 0.5 mA cm⁻², 0.5 mAh cm⁻²; b) cycling performance of Zn/Zn symmetrical cells in 3 M ZnSO₄ $\rm H_2O/EG$ hybrid electrolytes with various EG contents (0, 10, 68 vol%) at 5 mA cm⁻², 0.5 mAh cm⁻²; c) cycling lifespan and d) over-potential at the 10th cycle of the Zn/Zn cells as a function of EG content ranging from 0 to 68 vol%; and e) CE obtained from Zn/Cu cells with different electrolytes.

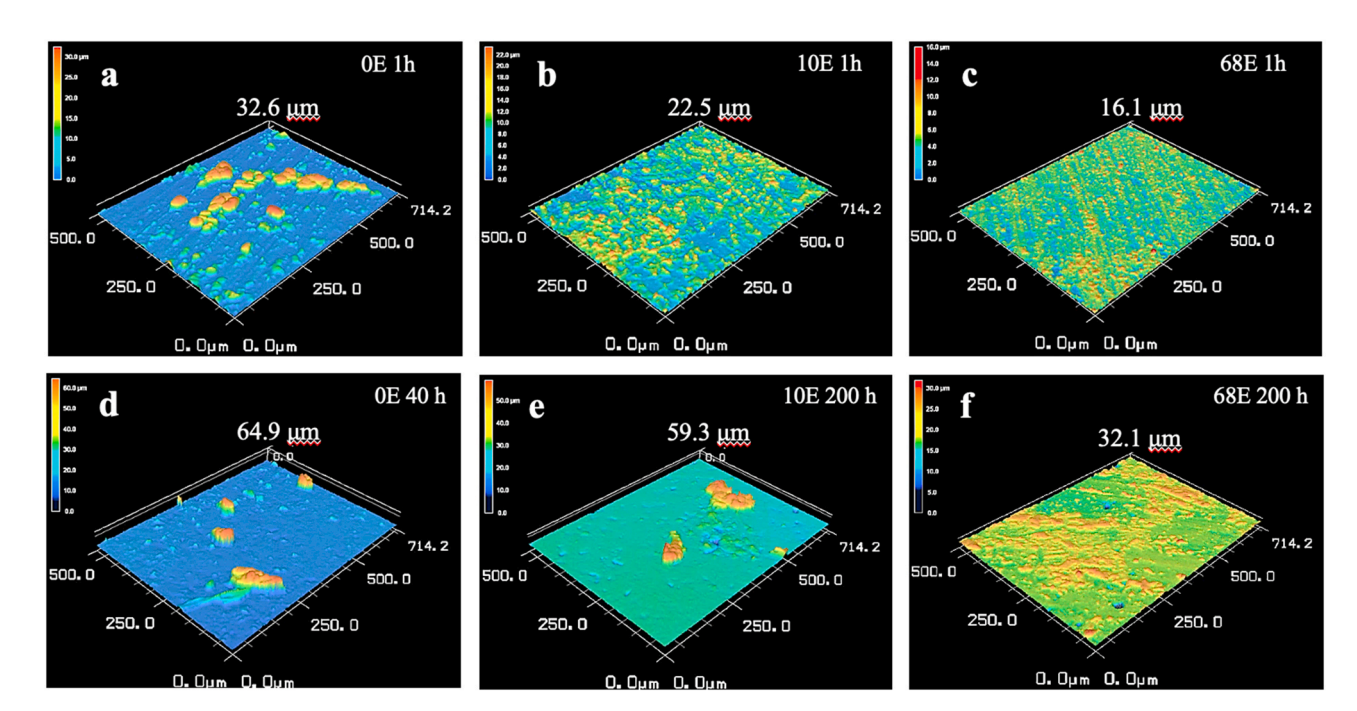


Fig. 2. LCSM images of Zn plate at different cycling time in 3 M ZnSO₄/ H_2O / EG electrolytes. LCSM images of Zn plate after plating at 0.5 mA cm⁻² for 1 h in a) 0E, b) 10E, and c) 68E electrolytes; d) LCSM images of Zn plate after cycling at 0.5 mA cm⁻² for 40 h in 0E electrolytes; and LCSM images of Zn plate after cycling at 0.5 mA cm⁻² for 200 h in e) 10E and f) 68E electrolytes.

measurements, three strong peaks arise for 0E electrolyte at $8.13^{\circ},\,16.31^{\circ}$ and 24.54° (Fig. S11), indicative of the by-product $Zn_4(OH)_6.$ $SO_40.5~H_2O~[30]$, whereas substantially weaker peaks are displayed for the 10E and 68E electrolytes. The EDS mapping of the dendrite also shows the distribution of Zn, S and O elements in the bulk dendrite (Fig. S12), which confirms the existence of the by-product [31,32]. Apparently, side-reactions and subsequent generation of by-products are effectively eliminated by the addition of EG in the electrolytes. Given that the symbiosis of Zn tips and the by-product is likely to accelerate the Zn dendrite growth process [33], the double role played by EG in promoting both uniform Zn nucleation and side-reaction resistance may account for its success in diminishing the dendrite formation.

2.3. Tuning Zn²⁺ coordination with EG

According to previous literatures [34–36], the scenario of Zn deposition during cycling can be described as follows (Fig. 3a). (i) A presumable $[{\rm Zn}({\rm H_2O})_m({\rm EG})_n]^{2+}$ coordination complex diffuses to the Zn/electrolyte interface under electric field. (ii) Electrons are injected from Zn anode to the attached complex via tunneling, reducing the ${\rm Zn}^{2+}$ ion and breaking the solvation sheath. (iii) ${\rm Zn}^{\delta+}$ ($\delta<2$) is released to the Zn anode surface and anchored at undercoordinated sites. We believe that EG in the ${\rm Zn}^{2+}$ -solvation sheath can exert considerable influence on stages (i) and (ii), and the detailed mechanistic insights will be revealed based on theoretical and experimental approaches.

Fig. S13 presents a summary of solvation energies with different Zn^{2+} -solvation sheath using ab initio calculations. The solvation energy associated with the formation of $[Zn(H_2O)_6]^{2+}$ is higher than $[Zn(H_2O)_m(EG)_n]^{2+}$, and the chelated Zn^{2+} ion in the form of $[Zn(EG)_3]^{2+}$ (Fig. 3b) appears to have the most negative solvation energy, suggesting

a stronger binding affinity of Zn^{2+} with EG than H_2O . It can be assumed that various $[Zn(H_2O)_m(EG)_n]^{2+}$ species coexists in the EG-containing electrolytes, and the larger radii of these complexes than that of $[Zn(H_2O)_6]^{2+}$ would contribute to a more sluggish diffusion of the former. This is further verified by the ionic conductivities of different electrolytes shown in Fig. 3c. Note that the conductivity of Zn^{2+} in 68E electrolyte at 25 °C is nearly one order of magnitude lower than that of 0E electrolyte, which may prevent the rapid growth of dendrites and benefit a uniform distribution of Zn deposits on the anode surface with a high-EG-content electrolyte.

While a relatively low diffusivity of Zn²⁺ ions in stage (i) can regulate Zn dendrite growth, a bulkier and more rigid coordination complex of $[Zn(H_2O)_m(EG)_n]^{2+}$ will concomitantly lead to increased nucleation over-potential (NOP), thus affecting the kinetics in stage (ii). On one hand, a comparatively low solvation energy of Zn²⁺ in EG-containing electrolytes means a high Zn²⁺-EG interaction and a rigid coordination linkage, which elevates the barrier for the dissolution of Zn²⁺. On the other hand, the radii of complexes like [Zn(EG)₃]²⁺ are much greater than that of $[Zn(H_2O)_6]^{2+}$ (Fig. 3b), indicating that when the complex attaches to the anode surface, the Zn²⁺ ion will be more distant from the surface in the case of $[Zn(EG)_3]^{2+}$. Consequently, electron tunneling is reduced, and it will consume a larger amount of energy to break the Zn²⁺-solvation sheath [37], accounting for the increased NOP shown in Fig. 3d (working electrode: stainless steel). This effect can be termed the "steric hindrance". The high NOP corresponds to a strong driving force for nucleation and will more probably yield fine-grained deposits, whereas the low NOP can have the opposite effect, that is, the deposits quickly grow into dendrites due to tip effect [38,39]. By virtue of the high NOP, the Zn deposition morphology in aqueous electrolytes can be significantly optimized with the addition of EG. Since the average

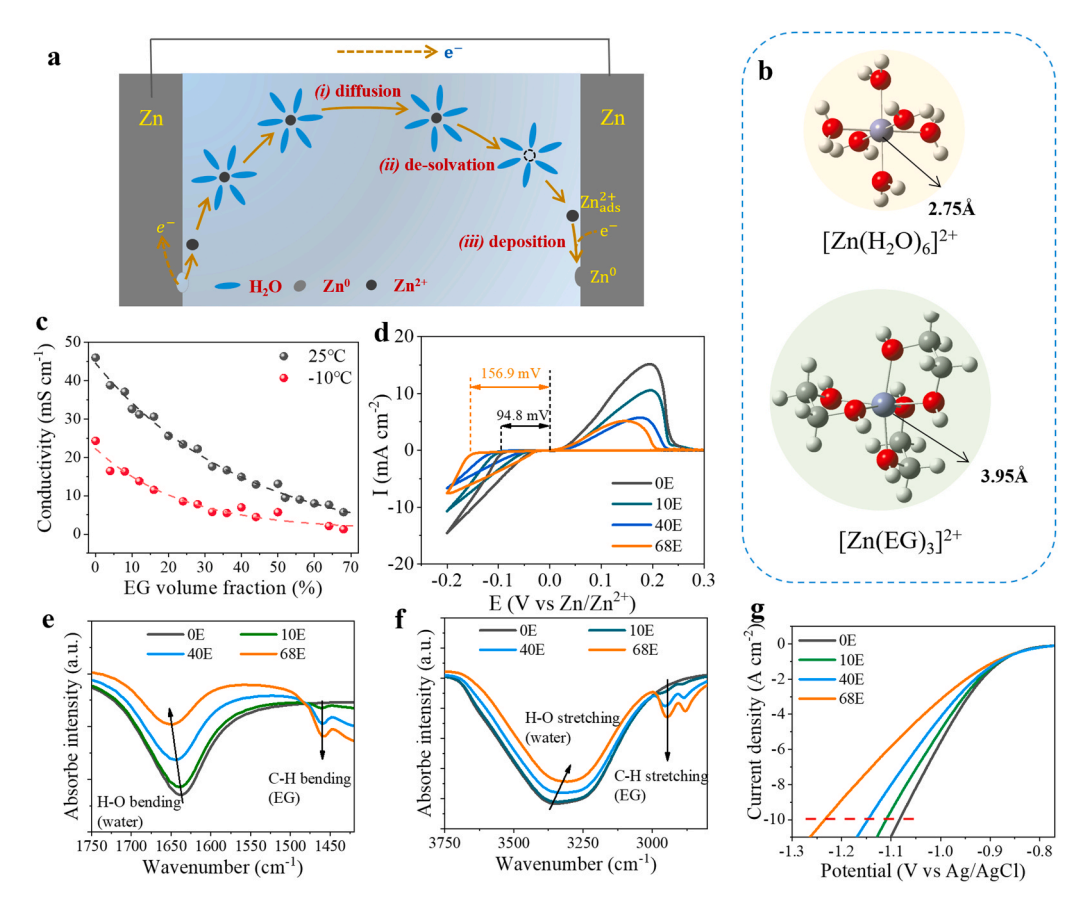


Fig. 3. a) Schematic illustration of Zn deposition processes; b) coordination complexes of $Zn[(H_2O)_6]^{2+}$ and $Zn[(EG)_3]^{2+}$; c) ionic conductivity of different H_2O/EG hybrid electrolyte at temperature of 25 °C and -10 °C; d) cyclic voltammetry curves of the bare Zn plate anodes in different electrolytes; e) and f) FTIR spectrum results of different electrolytes; g) HER curves in different electrolytes.

number of EG neighbors around a $\rm Zn^{2+}$ ion is presumably dictated by the EG content in the electrolyte, it can be expected that significant steric hindrance for $[\rm Zn(H_2O)_m(EG)_n]^{2+}$ complexes would characterize the high-EG-content electrolytes, thereby rendering the sluggish behavior of $\rm Zn^{2+}$ desolvation. This rationalizes our observation that higher EG content generally results in better cycling performance while accompanying larger polarization (Figs. 1c and 1d). Some researchers consider that EG functions as "water blocker" [23] outside of the primary hydrated solvation sheath of $\rm Zn^{2+}$ ([$\rm Zn(H_2O)_6]^{2+}$), but no evidence was given. With strong experiment and computation results, we provide a totally different complex structure ([$\rm Zn(H_2O)_m(EG)_n]^{2+}$), and propose the idea of tuning $\rm Zn^{2+}$ coordination environment by low-cost additives so as to suppress Zn dendrite formation.

The coordination of EG to ${\rm Zn}^{2+}$ ions could facilitate ${\rm H}_2{\rm O}{\rm -H}_2{\rm O}$ hydrogen bond formation, because the ${\rm H}_2{\rm O}$ molecules in the aqua ion ${\rm [Zn(H}_2{\rm O)}_6]^{2+}$ are now liberated into the bulk solution phase [40]. This is substantiated by the FTIR spectra in Figs. 3e and 3f, where the blueshift of the H–O bending vibration and the red-shift of the H–O stretching vibration are clearly discernible [41,42]. Owing to the increase in the number of hydrogen bonds, the HER activity is decreased when EG is in the electrolyte, as shown in Fig. 3g and Fig. S14. Moreover, in 0E electrolyte, the coordinating ${\rm H}_2{\rm O}$ molecules around ${\rm Zn}^{2+}$ will be confined close to the surface when the ${\rm Zn}^{2+}$ ion is about to settle down for deposition. This will promote the electron transfer to the ${\rm H}_2{\rm O}$ molecules and enhance the HER activity. In contrast, a decreased number of coordinating ${\rm H}_2{\rm O}$ as well as a more remote distance of [Zn ${\rm (H}_2{\rm O)}_m({\rm EG})_n]^{2+}$ to the surface would suggest a lower opportunity for side reactions, especially HER [43,44].

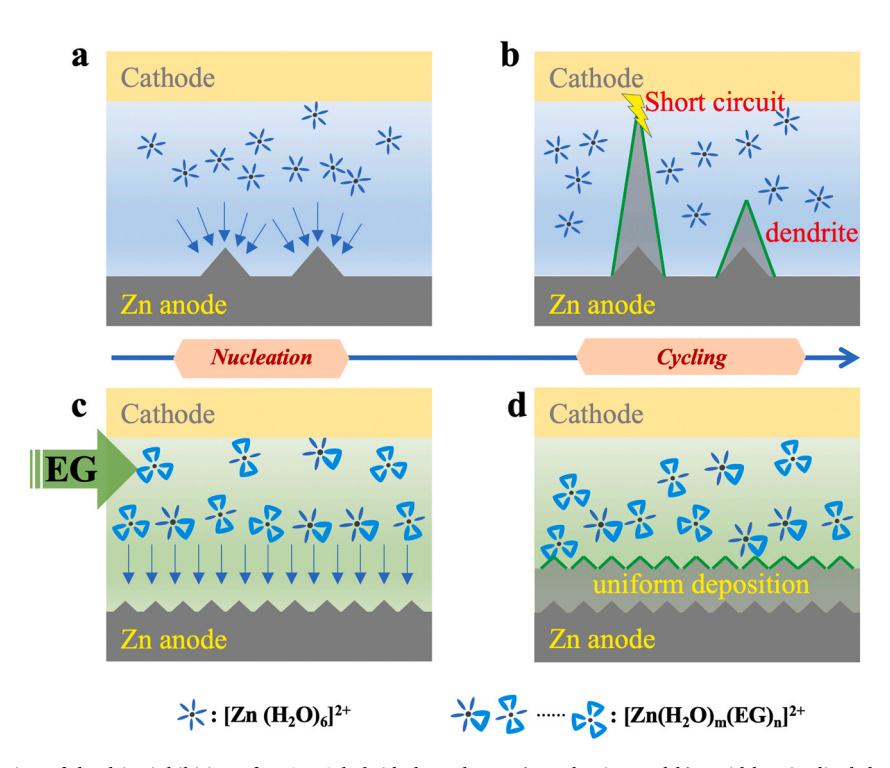
Based on the above discussions, we can speculate that the prolonged cycling lifespan of Zn/Zn cells in $\rm H_2O/EG$ hybrid electrolytes is mainly due to the combined effect of decreased diffusivity of $\rm Zn^{2+}$, increased NOP and lowered probability of side reactions. The schematic illustrations of Zn dendrite formation in EG-free and EG-containing electrolytes are depicted in Scheme 2. In the beginning of plating process, the Zn nuclei in $\rm H_2O/EG$ hybrid electrolyte are much smaller in size and larger in quantity as compared with the counterpart without EG (Schemes 2a,

2c). With further plating, the latter one will witness bulk porous coralloid dendrites grown up symbiotically with by-products from side reactions (Scheme 2b), followed by a rapid longitudinal growth of several large-size dendrites that penetrate through the separators and cause short-circuit failure. However, in H₂O/EG hybrid electrolyte, smooth and compact Zn deposits with minimal by-products are obtained even after long-term cycling (Scheme 2d), which guarantees the superior cycling lifespan of Zn/Zn cells.

As noted above, EG is a representative polyalcohol that provides a promising solution for dendrite suppression with balance of price, toxicity, viscosity, and solubility. Given that the hydroxyl groups act as the effective ligands replacing $\rm H_2O$ around the $\rm Zn^{2+}$ ion, the mechanistic insights could be extended to other types of alcohols shown in Fig. S1, which offers an excellent platform for tuning the coordination environment of $\rm Zn^{2+}$. We believe that the performance can be further improved by employing more sophisticatedly designed polyalcohol groups, though with the trade-off of higher price. Future work embodying a comparison between different alcohol-added electrolytes is therefore warranted.

2.4. Battery applications

To investigate the performance of $\rm H_2O/EG$ hybrid electrolyte in an actual full battery, we used $\rm Zn_x V_2O_5$ n $\rm H_2O$ (ZnVO) nanorods as the cathode material following the research by Kundu et al. [45]. We note that the layer structure of ZnVO (Fig. S15a) can permit reversible Zn intercalation and deintercalation. The porous nanorods with a typical size of ~800 nm in length and ~100 nm in diameter are characterized by TEM (Fig. S15b), and a uniform distribution of Zn, V and O elements is confirmed by EDS (Fig. S15c). The full ZnVO/Zn battery was assembled with bare Zn plate as anode, ZnVO as cathode, and a cellulose membrane as separator, in electrolytes with different concentration of EG. The cycling performances of the full batteries are shown in Fig. 4a. Though the anode is excessive in mass, the dendrite formation and the following short circuit determine the failure of the full battery. Cells with OE, 10E and 40E electrolytes fail after 18, 143 and 289 cycles, while



Scheme 2. Schematic illustration of dendrite inhibition of H_2O/EG hybrid electrolytes. a) Nucleation and b) rapid longitudinal dendrite growth after cycling in aqueous $ZnSO_4/H_2O$ electrolyte; c) nucleation and d) optimized Zn deposition morphology after cycling in $ZnSO_4/H_2O/EG$ hybrid electrolyte.

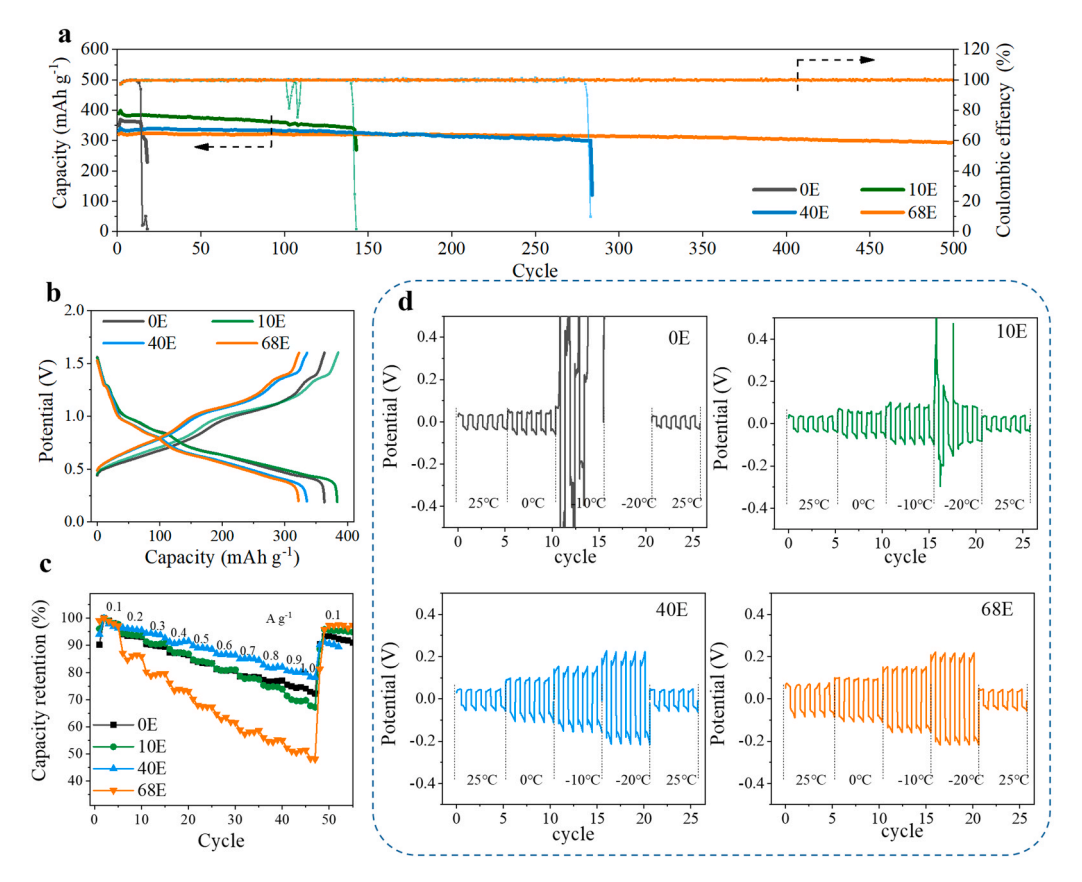


Fig. 4. Electrochemical performance of cells using H_2O/EG hybrid electrolytes. a) Cycling performances, b) charge/discharge profiles at 10th cycle, and c) rate capabilities of ZnVO/Zn full batteries with different electrolytes; and d) voltage profiles for Zn/Zn cells at different temperatures.

the one with 68E electrolyte can operate over 500 cycles with a high initial capacity of 329 mAh g $^{-1}$ (at 0.5 A g $^{-1}$) and a high capacity retention of 89.6%. Fig. 4b shows the charge/discharge curves of ZnVO/Zn batteries, which have similar profiles for all the electrolytes, indicating the preservation of Zn $^{2+}$ intercalation/deintercalation mechanism in ZnVO, regardless of the different electrolytes studied in this work. Presented in Fig. 4c, the addition of EG in the electrolyte would in general negatively affect the rate capability, for the stronger desolvation hindrance in hybrid electrolytes is infaust for cathodes kinetics. The weak rate performance in high-concentrated EG electrolytes is consistent with the sluggish kinetics of the $[\text{Zn}(\text{H}_2\text{O})_m(\text{EG})_n]^{2+}$ coordination complex. Therefore, a compromise between cycling lifespan and rate performance would have to be taken into account when designing coordination tuning of Zn^{2+} by EG (or other additives) in the electrolyte.

Differential scanning calorimetry (DSC) tests (Fig. S16), carried out to examine electrolyte freezing [46], reveal that the electrolytes containing 32–68 vol% EG remain in liquid state even at -50 °C. This can be ascribed to the anti-freezing property of EG solvent, and would allow for future applications of these electrolytes in extreme low-temperature environments [47]. To estimate the working temperature range of the Zn/Zn symmetric cells, the cycling performance at 0.5 mA cm⁻² under different temperatures is investigated, as shown in Fig. 4e. Cells with 40E and 68E electrolytes can operate effectively at temperature as low as −20 °C, whereas an open-circuit failure with sudden polarization occurs for 0E and 10E electrolytes at -10 °C and -20 °C, respectively, on account of the restricted diffusivity of Zn²⁺ ions in the frozen state of the aqueous solution. This result can be extended to ZnVO/Zn full battery, for which an impressive capacity of 100 mAh g⁻¹ at -20 °C is obtained using 68E electrolyte (Fig. S17). Non-flammability of the H2O/EG hybrid electrolyte was also tested by igniting the separator soaked in the 68E electrolyte by an alcohol burner (Fig. S18, supplementary video). The hybrid electrolyte does not catch fire even though EG is combustible, probably due to the relatively high ignition temperature of EG (418 °C) and the high concentration of incombustible Zn salt [48]. The above observation confirms that the cells employing $\rm H_2O/EG$ hybrid electrolyte can inherit the advantage of aqueous batteries in terms of safety issue.

Supplementary material related to this article can be found online at doi:10.1016/j.nanoen.2020.105478.

3. Conclusions

In summary, we have investigated the Zn dendrite inhibition strategy via tuning Zn²⁺ coordination environment in H₂O/EG hybrid electrolyte. In high-EG-content electrolytes, the solvation sheath of Zn^{2+} ions are dominated by EG molecules, which will constrain the diffusion of Zn²⁺, increase the over-potential for Zn deposition and suppress the parasitic reactions during cycling. All these factors synergistically enable uniform Zn nucleation and growth, thus resulting in dramatic improvement in cycling performances. Leveraging this feature, Zn/Zn cells with 3 M ZnSO₄/H₂O/68 vol% EG electrolyte achieves an ultralong cycling lifespan (2668 h at 0.5 mA cm⁻²), which is among the best for bare Zn anodes. The superior cyclability of H₂O/EG hybrid electrolyte is also demonstrated when coupled with ZnVO cathode, along with its anti-freezing and non-flammable characteristics. This low-cost electrolyte offers a promising strategy to prevent the detrimental dendrite growth in Zn anodes and will guide the development of next-generation electrolytes for ZIBs.

CRediT authorship contribution statement

Runzhi Qin¹: Conceptualization, Investigation, Writing - original draft. Yuetao Wang¹: Investigation. Mingzheng Zhang¹: DFT calculation. Yan Wang: Methodology. Shouxiang Ding: Resources. Aoye

Song: Resources. Haocong Yi: Formal analysis. Luyi Yang: Investigation. Yongli Song: Investigation. Yanhui Cui: Resources. Jian Liu: Resources. Ziqi Wang: Data Curation. Shunning Li*: Writing - review & editing. Qinghe Zhao*: Writing - original draft, Funding acquisition. Feng Pan*: Supervision, Project administration, Funding acquisition.

Declaration of Competing Interest

The authors declare that they have no known competing financial interests or personal relationships that could have appeared to influence the work reported in this paper.

Acknowledgements

This work was financially supported by Basic and Applied Basic Research Foundation of Guangdong Province, China (No. 2019A1515110094), and Shenzhen Natural Science Foundation, China (No. JCYJ20190813110605381).

Appendix A. Supporting information

Supplementary data associated with this article can be found in the online version at doi:10.1016/j.nanoen.2020.105478.

References

- [1] H. Li, L. Ma, C. Han, Z. Wang, Z. Liu, Z. Tang, C. Zhi, Nano Energy 62 (2019) 550–587.
- [2] B. Tang, L. Shan, S. Liang, J. Zhou, Energy Environ. Sci. 12 (2019) 3288–3304.
- [3] N. Zhang, X. Chen, M. Yu, Z. Niu, F. Cheng, J. Chen, Chem. Soc. Rev. 4 (2020), 771–17.
- [4] C. Xu, B. Li, H. Du, F. Kang, Angew. Chem. Int. Ed. 51 (2012) 933-935.
- [5] Q. Zhao, S. Ding, A. Song, R. Qin, P. Feng, Chin. J. Struct. Chem. 39 (2020) 388–394.
- [6] Q. Zhao, X. Chen, Z. Wang, L. Yang, R. Qin, J. Yang, Y. Song, S. Ding, M. Weng, W. Huang, J. Liu, W. Zhao, G. Qian, K. Yang, Y. Cui, H. Chen, F. Pan, Small 15 (2019), 1904545.
- [7] M. Liu, Q. Zhao, H. Liu, J. Yang, X. Chen, L. Yang, Y. Cui, W. Huang, W. Zhao, A. Song, Y. Wang, S. Ding, Y. Song, G. Qian, H. Chen, F. Pan, Nano Energy 189 (2019), 116367-840.
- [8] J. Li, K. McColl, X. Lu, S. Sathasivam, H. Dong, L. Kang, Z. Li, S. Zhao, A.G. Kafizas, R. Wang, D.J.L. Brett, P.R. Shearing, F. Corà, G. He, C.J. Carmalt, I.P. Parkin, Adv. Energy Mater. 8 (2020), 2000058–14.
- [9] D. Kundu, S. Hosseini Vajargah, L. Wan, B. Adams, D. Prendergast, L.F. Nazar, Energy Environ. Sci. 11 (2018) 881–892.
- [10] Z. Liu, G. Pulletikurthi, F. Endres, ACS Appl. Mater. Inter. 8 (2016) 12158-12164.
- [11] J. Xiang, L. Yang, L. Yuan, K. Yuan, Y. Zhang, Y. Huang, J. Lin, F. Pan, Y. Huang, Joule 3 (2019) 2334–2363.
- [12] V. Yufit, F. Tariq, D.S. Eastwood, M. Biton, B. Wu, P.D. Lee, N.P. Brandon, Joule 3 (2019) 485–502.
- [13] H. Jia, Z. Wang, B. Tawiah, Y. Wang, C.-Y. Chan, B. Fei, F. Pan, Nano Energy 70 (2020), 104523.
- [14] Q. Yang, G. Liang, Y. Guo, Z. Liu, B. Yan, D. Wang, Z. Huang, X. Li, J. Fan, C. Zhi, Adv. Mater. 31 (2019), e1903778.
- [15] Z. Wang, J. Hu, L. Han, Z. Wang, H. Wang, Q. Zhao, J. Liu, F. Pan, Nano Energy 56 (2019) 92–99.
- [16] M. Liu, L. Yang, H. Liu, A. Amine, Q. Zhao, Y. Song, J. Yang, K. Wang, F. Pan, ACS Appl. Mater. Inter. 11 (2019) 32046–32051.
- [17] Y. Cui, Q. Zhao, X. Wu, X. Chen, J. Yang, Y. Wang, R. Qin, S. Ding, Y. Song, J. Wu, K. Yang, Z. Wang, Z. Mei, Z. Song, H. Wu, Z. Jiang, G. Qian, L. Yang, F. Pan, Angew. Chem. 39 (2020) 388.
- [18] W. Guo, Z. Cong, Z. Guo, C. Chang, X. Liang, Y. Liu, W. Hu, X. Pu, Energy Storage Mater. 30 (2020) 104–112.
- [19] M. Chamoun, B.J. Hertzberg, T. Gupta, D. Davies, S. Bhadra, B.V. Tassell, C. Erdonmez, D.A. Steingart, NPG Asia Mater. 7 (2015) e178–e178.
- [20] Z. Cai, Y. Ou, J. Wang, R. Xiao, L. Fu, Z. Yuan, R. Zhan, Y. Sun, Energy Storage Mater. 27 (2020) 205–211.
- [21] S.-B. Wang, Q. Ran, R.-Q. Yao, H. Shi, Z. Wen, M. Zhao, X.-Y. Lang, Q. Jiang, Nat. Commun. 11 (2020) 1634.
- [22] W. Xu, K. Zhao, W. Huo, Y. Wang, G. Yao, X. Gu, H. Cheng, L. Mai, C. Hu, X. Wang, Nano Energy 62 (2019) 275–281.
- [23] N. Wang, Y. Yang, X. Qiu, X. Dong, Y. Wang, Y. Xia, ChemSusChem (2020) cssc,202001750-11.
- [24] C. Zhang, J. Holoubek, X. Wu, A. Daniyar, L. Zhu, C. Chen, D.P. Leonard, I. A. Rodríguez-Pérez, J.-X. Jiang, C. Fang, X. Ji, Chem. Commun. 54 (2018) 14097–14099.
- [25] F. Wang, O. Borodin, T. Gao, X. Fan, W. Sun, F. Han, A. Faraone, J.A. Dura, K. Xu, C. Wang, Nat. Mater. 17 (2018) 543–549.

- [26] Y. Cui, Q. Zhao, X. Wu, Z. Wang, R. Qin, Y. Wang, M. Liu, Y. Song, G. Qian, Z. Song, L. Yang, F. Pan, Energy Storage Mater. 27 (2020) 1–8.
- [27] H. Yang, Z. Chang, Y. Qiao, H. Deng, X. Mu, P. He, H. Zhou, Angew. Chem. Int. Ed. 59 (2020) 9377–9381.
- [28] L. Wang, K.-W. Huang, J. Chen, J. Zheng, Sci. Adv. 5 (2019), eaax4279.
- [29] H. He, H. Tong, X. Song, X. Song, J. Liu, J. Mater. Chem. A 8 (2020) 7836-7846.
- [30] C. Deng, X. Xie, J. Han, Y. Tang, J. Gao, C. Liu, X. Shi, J. Zhou, S. Liang, Adv. Funct. Mater. 30 (2020), 2000599.
- [31] D. Han, S. Wu, S. Zhang, Y. Deng, C. Cui, L. Zhang, Y. Long, H. Li, Y. Tao, Z. Weng, Q.H. Yang, F. Kang, Small 5 (2020) 2001736–2001737.
- [32] R. Yuksel, O. Buyukcakir, W.K. Seong, R.S. Ruoff, Adv. Energy Mater. 10 (2020),
- [33] L. Ma, S. Chen, N. Li, Z. Liu, Z. Tang, J.A. Zapien, S. Chen, J. Fan, C. Zhi, Adv. Mater. 32 (2020), 1908121.
- [34] J. Hu, W. Ren, X. Chen, Y. Li, W. Huang, K. Yang, L. Yang, Y. Lin, J. Zheng, F. Pan, Nano Energy 74 (2020), 104864.
- [35] R. Qin, W. Yan, Q. Zhao, Y. Kai, P. Feng, Chin. J. Struct. Chem. 39 (2020) 605–614.
- [36] W. Yang, X. Du, J. Zhao, Z. Chen, J. Li, J. Xie, Y. Zhang, Z. Cui, Q. Kong, Z. Zhao, C. Wang, Q. Zhang, G. Cui, Joule (2020) 1–52.
- [37] A. Pei, G. Zheng, F. Shi, Y. Li, Y. Cui, Nano Lett. 17 (2017) 1132-1139.
- [38] Z. Zhao, J. Zhao, Z. Hu, J. Li, J. Li, Y. Zhang, C. Wang, G. Cui, Energy Environ. Sci. 12 (2019) 1938–1949.
- [39] S.-S. Chi, Q. Wang, B. Han, C. Luo, Y. Jiang, J. Wang, C. Wang, Y. Yu, Y. Deng, Nano Lett. 20 (2020) 2724–2732.
- [40] J. Zheng, G. Tan, P. Shan, T. Liu, J. Hu, Y. Feng, L. Yang, M. Zhang, Z. Chen, Y. Lin, J. Lu, J.C. Neuefeind, Y. Ren, K. Amine, L.-W. Wang, K. Xu, F. Pan, Chem 4 (2018) 2872–2882.
- [41] J. Xie, Z. Liang, Y.-C. Lu, Nat. Mater. 451 (2020) 652-658.
- [42] J. Zhang, P. Zhang, K. Ma, F. Han, G. Chen, X. Wei, Sci. China Ser. B 51 (2008) 420–426.
- [43] F. Mo, G. Liang, Q. Meng, Z. Liu, H. Li, J. Fan, C. Zhi, Energy Environ. Sci. 12 (2019) 706–715.
- [44] Q. Zhao, J. Yang, M. Liu, R. Wang, G. Zhang, H. Wang, H. Tang, C. Liu, Z. Mei, H. Chen, F. Pan, ACS Catal. 8 (2018) 5621–5629.
- [45] D. Kundu, B.D. Adams, V. Duffort, S.H. Vajargah, L.F. Nazar, Nat. Energy 1 (2016), 928–928.
- [46] Q. Nian, J. Wang, S. Liu, T. Sun, S. Zheng, Y. Zhang, Z. Tao, J. Chen, Aqueous batteries operated at -50 °C, Angew. Chem. 131 (2019) 17150-17155.
- [47] N. Chang, T. Li, R. Li, S. Wang, Y. Yin, H. Zhang, X. Li, Energy Environ. Sci. 2 (2020) 1–10.
- [48] K. Zhang, L. Zong, Y. Tan, Q. Ji, W. Yun, R. Shi, Y. Xia, Carbohydr. Polym. 136 (2016) 121–127.



Runzhi Qin received his B.S. degree from University of Science and Technology of Beijing (USTB, China) in 2013, and earned Ph.D. degree from the School of Materials Science and technology at USTB in 2019, majoring in the electrochemical corrosion behavior of iron-based alloys, under the supervision of Prof. Minxu Lu. Dr. Qin is now a post-doctor in Prof. Feng Pan's group in School of Advanced Materials, Peking University Shenzhen Graduate School, China. His research interests mainly focus on the key materials and technologies for zinc-based batteries.



Yuetao Wang received his B.E. degree from the College of Chemistry and Molecular Engineering in Peking University (PKU, China) in 2018. He is currently a Ph.D. degree candidate under the supervision of Prof. Feng Pan in School of Advanced Materials, Peking University Shenzhen Graduate School, China. His research interests focus on the aqueous zinc ion batteries, especially on the vanadium-based cathode materials.



Mingzheng Zhang received his B.S. degree in Chemistry from Xiamen University in 2019. Currently, he works under the supervision of Prof. Jiaxin Zheng and Prof. Feng Pan as a Ph. D candidate at School of Advanced Materials, Peking University Shenzhen Graduate School, China. His research interests mainly focus on first principle calculation of clusters and battery materials.



Luyi Yang received his B.S. degree from the Department of Chemistry at Xiamen University (China) in 2010, and earned Ph.D. degree from the School of Chemistry at Southampton University (U.K.) in 2015 under the supervision of Prof. John Owen. Dr. Yang is currently a researcher at the School of Advanced Materials, Peking University Shenzhen Graduate School. His research interests mainly focus on the investigation of key materials in lithium batteries including solid-state electrolytes, layered oxide cathode materials and binders for Si anodes.



Yan Wang obtained B.S. degree from College of Chemistry and Molecular Engineering, Peking University in 2018. He is currently a postgraduate student in Prof. Pan's group at the School of Advanced Materials, Peking University Shenzhen Graduate School. His research interests are synthesis of novel materials for energy storage and in situ battery characterization techniques.



Yongli Song received his B.S. degree from Harbin Institute of Technology (HIT, China) in 2010, and earned Ph.D. degree from physics department at HIT in 2017, majoring in the high dielectric constant materials, under the supervision of Prof. Yu Sui. Dr. Song is now associate researcher in School of Advanced Materials, Peking University Shenzhen Graduate School, China. His research interests mainly focus on solid state lithium metal battery and solid-state electrolytes.



Shouxiang Ding graduated from South China University of Technology (SUCT, China) and received his B.S. degree from the School of Chemistry and Chemical Engineering in 2019. He is currently a postgraduate student in Prof. feng Pan's group at the school of Advanced Materials, Peking University Shenzhen Graduate School. His research interests focus on the cathode materials of aqueous zinc ion battery.



Yanhui Cui received his B.E. degree in Packing Engineering from Zhengzhou University, China in 2010. After which he completed his Master's and Ph.D. degree under the supervision of Prof. Andrew Baker and Junwei Wu in Materials Science at Harbin Institute of Technology (Shenzhen) in 2014 and 2018, respectively. Now, Dr. Cui is a postdoctoral researcher in School of Advanced Materials, Peking University Shenzhen Graduate School (China) in Prof. Feng Pan's group. His research interests focus on energy storage/conversion fields.



Aoye Song graduated with a B.S. degree in the College of Chemistry and Molecular Engineering of Peking University (PKU, China) in 2018. During his undergraduate studies, he majored in the modification of NMC material lithium-ion batteries under the guidance of Prof. Henghui Zhou. Aoye Song is now pursuing a master's degree with Prof. Feng Pan at the School of Advanced Materials, Peking University Shenzhen Graduate School, China. His main research interests are advanced energy storage materials, especially in the areas of zinc-ion aqueous batteries.



Jian Liu received his B.E. degree in from Jinan University in 2007, and earned Master's degree from School of Material Physics and Chemistry in 2010 under the supervision of Prof. Xierong Zeng. Mr. Liu is now an engineer in School of Advanced Materials, Peking University Shenzhen Graduate School, China. His research interests mainly focus on the key material of crystalline silicon solar cell.



Haocong Yi received his B.S. degree from Huazhong University of Science and Technology (HUST, China) in 2018. He is currently a Ph.D. degree candidate under the supervision of Prof. Feng Pan in School of Advanced Materials, Peking University Shenzhen Graduate School, China. His research interests focus on the aqueous zinc ion batteries.



Ziqi Wang, professor of College of Chemistry and Materials Science, Jinan University, received his Ph.D. degree under the supervision of Prof. Guodong Qian at Zhejiang University in 2016. Before he joined Jinan University, he worked as a post-doctoral researcher at Peking University Shenzhen Graduate School and Hong Kong Polytechnic University since 2017 and 2019, respectively. His research interests focus on metalorganic frameworks (MOFs) and their applications in electrochemical energy storage.



Shunning Li received his B.E. degree in 2013 and Ph.D. degree in 2018 from School of Materials Science and Engineering, Tsinghua University, China. Currently, he is an assistant research fellow at the School of Advanced Materials, Peking University, Shenzhen Graduate School, China. His research interest focuses on the first-principles design of energy storage materials and heterogeneous catalysts.



Feng Pan, Chair-Professor, Founding Dean of School of Advanced Materials, Peking University Shenzhen Graduate School, Director of National Center of Electric Vehicle Power Battery and Materials for International Research, received his B.S. degree from Dept. Chemistry, Peking University in 1985 and Ph.D. from Dept. of P&A Chemistry, University of Strathclyde, U.K. with "Patrick D. Ritchie Prize" for the best Ph.D. in 1994. Prof. Pan has been engaged in fundamental research of structure chemistry, exploring "Material Gene" for Li-ion batteries and developing novel energy conversion-storage materials & devices. He also received the 2018 ECS Battery Division Technology Award.



Qinghe Zhao received his B.S. degree from University of Science and Technology of Beijing (USTB, China) in 2010, and earned Ph.D. degree from the School of Advanced Materials at USTB in 2016, majoring in the electrochemical corrosion behavior of iron-based alloys, under the supervision of Prof. Minxu Lu. Dr. Zhao is now associate researcher in School of Advanced Materials, Peking University Shenzhen Graduate School, China. His research interests mainly focus on the key materials and technologies for energy storage and conversion applications, including electro-catalyst, zinc ion and sodium ion batteries.